

## ARTICLE

# Analysis and evaluation of direct shear tests on concrete joints in hydraulic structures

Jan P. Höffgen<sup>1</sup>  | Viktória Malárics-Pfaff<sup>2</sup> | Doris B. Wengrzik<sup>1</sup> | Frank Dehn<sup>1</sup>

<sup>1</sup>Institute of Concrete Structures and Building Materials, Karlsruhe Institute of Technology, Karlsruhe 76131, Germany

<sup>2</sup>Federal Waterways Engineering and Research Facility, Structural Engineering, Karlsruhe 76187, Germany

## Correspondence

Jan P. Höffgen, Karlsruhe Institute of Technology, Institute of Concrete Structures and Building Materials, Gotthard-Franz-Str. 3, Karlsruhe, 76131, Germany.

Email: [jan.hoeffgen@kit.edu](mailto:jan.hoeffgen@kit.edu)

## Funding information

Federal Ministry for Digital and Transport: BMVI-Expertennetzwerk Wissen - Können - Handeln, Grant/Award Number: B3951.03.04.70014

## Abstract

Neither the shear transfer behavior of unreinforced hydraulic concrete structures nor experimental procedures for its determination have been standardized in recent building codes and regulations. This poses uncertainty for the assessment of the integrity of hydraulic structures. This paper adapts direct shear tests, which are an established method in rock mechanics, for the assessment of unreinforced concrete joints and expands the evaluation method through recognizing surface inclination as a contribution to the coefficient of friction. The evaluation is subsequently performed on direct shear test results performed on specimens taken from a lock built in the early 20th century. Based on the initial state of the concrete joints—intact or cracked bond—results for the basic friction angle and the inclination angle are discussed. Using entire shear stress-deformation-curves as opposed to singular values was found to yield more stable results of shear transfer parameters and additional insight on the validity of the test.

## KEYWORDS

concrete, dilation, direct shear test, hydraulic structures, joint, shear

## 1 | INTRODUCTION

Hydraulic structures like dams, locks and weirs often consist of unreinforced concrete and are required to transfer horizontal loads such as hydraulic and earth pressure. Insufficient structural resistance may lead to the sliding of entire concrete blocks, typically resulting in large deformations. Therefore, the shear transfer behavior of concrete joints plays a special role in the stability and load bearing capacity of such structures.

The shear resistance in concrete joints as specified in DIN EN 1992-1-1:2011-01<sup>1</sup> generally comprises three main mechanisms: adhesion, friction and reinforcement, the latter consisting of clamping and dowel effect. In unreinforced structures with potentially cracked joints subjected to varying loads, clamping and dowel effect must and adhesion should be considered negligible, leaving friction as the sole mechanism of load transfer. *fib* Model Code for Concrete Structures 2010<sup>2</sup> describes such cases as rigid bond-slip behavior, however, neglecting the large shear deformations occurring in hydraulic structures without their structural integrity being jeopardized. Therefore, knowledge and understanding of the realistic shear load bearing behavior and, specifically, of the friction coefficient,  $\mu$ , is of paramount importance.

Discussion on this paper must be submitted within two months of the print publication. The discussion will then be published in print, along with the authors' closure, if any, approximately nine months after the print publication.

This is an open access article under the terms of the [Creative Commons Attribution-NonCommercial-NoDerivs](https://creativecommons.org/licenses/by-nc-nd/4.0/) License, which permits use and distribution in any medium, provided the original work is properly cited, the use is non-commercial and no modifications or adaptations are made.

© 2023 The Authors. *Structural Concrete* published by John Wiley & Sons Ltd on behalf of International Federation for Structural Concrete.

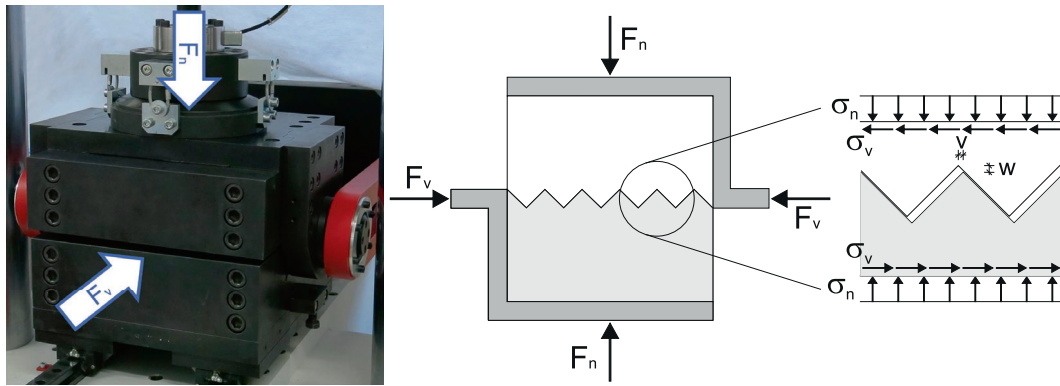


**FIGURE 1** Left: Direct shear test setup in the building materials laboratory of the German Federal Waterways Engineering and Research Institute (BAW); right: schematic sample loading with nomenclature of deformations, forces and stresses.

As there is no standardized method to determine the shear behavior of concrete joints, the interpretation of friction parameters from literature and experiments is further complicated. Therefore, this paper presents an analytical method to determine the shear resistance of concrete joints from direct shear tests and discusses evaluation approaches as groundwork for future research.

Following Coulomb's Law (Equation (1)),  $\mu$  depicts the ratio between a shear force  $F_v$  required to start or maintain a parallel movement of two objects and a compressive force normal to the shear plane  $F_n$ .

$$F_v = F_n \times \mu \quad (1)$$

The friction coefficient depends on material combination as well as on surface topology and assumes values between 0.5 and 1.0 for designing joints in concrete structures. Experimentally determined coefficients of friction appear to be dependent on the method and testing parameters, such as joint size, shearing rate or stress distribution, and should therefore be interpreted with caution.<sup>3</sup> In general,  $\mu$  is regarded as stress-invariant, although there is some disagreement in literature.<sup>3-7</sup> Especially for high stress levels, friction gradually transitions into a failure of the surrounding material when surface asperities are shorn off. For practical reasons, building codes such as DIN EN 1992-1-1:2011-01<sup>1</sup> use an upper stress limit to account for the cohesive shear failure of the surrounding concrete instead of a gradual transition.

The friction coefficient can be illustrated as the tangent of a friction angle,  $\varphi$ , where  $\varphi$  is the angle at which a shear plane needs to be tilted for a movement to start.

$$\mu = \tan \varphi \quad (2)$$

Another way to determine  $\varphi$  is through direct shear tests, where a constant vertical compressive force is applied to a specimen with a horizontal joint (Figure 1).<sup>8</sup>

By measuring the horizontal shear force,  $F_v$ , necessary for increasing a relative horizontal displacement,  $v$ , the basic friction coefficient can be obtained as the ratio of the residual shear force and the constant normal force,  $F_n$ . Direct shear tests have been widely used in the research of unreinforced concrete.<sup>9-15</sup> Variations focus on different approaches to negate or counteract bending moments caused by load transfer. Adaptions of the test setup can also include the addition of reinforcement.<sup>16-19</sup>

In contrast to theory, shear tests on inclined or rough concrete specimens rarely yield asymptotic residual shear forces, thus requiring the additional consideration of shear dilation,  $w$ , in Equation (3).

$$\mu = \tan(\varphi + i) \quad \text{with} \quad i = \arctan \frac{dw}{dv} \quad (3)$$

The dilation angle is the angle between relative horizontal ( $v$ ) and vertical ( $w$ ) deformations of the upper and lower halves of the shear test specimen and depends on the effective surface topology, that is,  $i = 0^\circ$  for perfectly smooth and level shear planes. Splitting the friction coefficient in a topology-dependent and a material-dependent part allows for a more in-depth investigation of the shear transfer behavior.<sup>7,13</sup> This is essential for the assessment of the load bearing capacities of concrete hydraulic structures for their resemblance with rock joints. The direct shear test is an established evaluation method for assessing the sliding stability of rock discontinuities.<sup>3</sup> The effective inclination depends on surface topology, represented by a **joint roughness coefficient** (JRC) and the ratio of **joint wall compressive strength** at the discontinuity (JCS) and normal stress  $\sigma_n$  (Equation (4)).<sup>5</sup>

$$i = \text{JRC} \times \lg \left( \frac{\text{JCS}}{\sigma_n} \right) \quad (4)$$

Since the joint roughness coefficient requires a qualitative comparison of the surface topology profile with

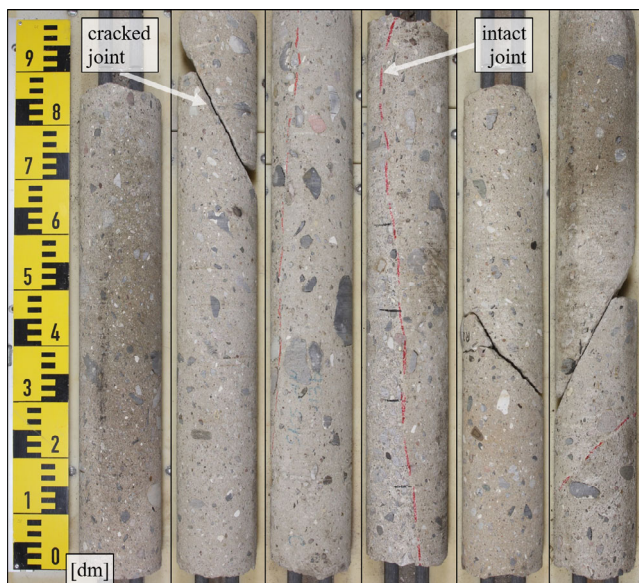


**FIGURE 2** Selected drill-cores with and without joints obtained from a Northern-German lock built in the early 20th century. Joints are either cracked or have been marked in red.

tabulated examples, research has focused on calculating JRC from quantitative roughness parameters, finding a good correlation of JRC and the root-mean-square of the asperity angles  $Z_2$  of the surface profile (Equation (5)).<sup>20</sup>

$$JRC = 32.2 + 32.47 \times \lg Z_2 \quad \text{with} \quad (5)$$

$$Z_2 = \sqrt{\frac{1}{N} \sum_{i=1}^N \left( \frac{y_{i-1} - y_i}{x_{i-1} - x_i} \right)^2}$$

where a linear surface profile is divided into  $N$  sections with a length of  $\Delta x = x_{i-1} - x_i$  with  $y_i$  as the distance of the profile line from the center line at each coordinate  $x_i$ . A refined expression takes only positive inclinations of surface elements into account, introducing a maximum contact coefficient and substituting the compressive strength for tensile strength, as shearing-off of asperities is caused by local tensile failure.<sup>21</sup>

Due to the differences between rock discontinuities and concrete joints, especially regarding roughness and heterogeneity, the application of Equations (4) and (5) on hydraulic structures requires additional research. As a first step, the presented results focus on methods for separating basic friction and inclination (compare Equation (3)).

## 2 | EXPERIMENTAL WORK

For the investigation of the shear transfer behavior of concrete joints in the present study, 76 direct shear tests were carried out in the building materials laboratory of

the German Federal Waterways Engineering and Research Institute (BAW). These 76 specimens were produced from 45 drill-cores with a diameter of 150 mm taken from a lock built in Northern Germany in the early 20th century as part of a large-scale condition evaluation.<sup>22</sup> Prior testing, drill-cores were sampled and categorized, see Figure 2. The bulk material was tamped concrete with a maximum aggregate size from 10 to 110 mm. Half of the drill-cores each consisted of gravel- or crushed-stone-concrete and had clearly visible deposits around their aggregates, indicating contamination. Flint and chalk were found in all drill-cores and opal sandstone in about half of them. Already visible alkali-silica-reaction-products could be detected in 24 drill-cores. Of the 76 specimens for shear testing, 51 were with intact bond and 25 were cracked. Their distribution within the lock did not follow any definite regularity. There were also drill-cores with two independent joints, one intact and one cracked bond. On specimens without joints compressive and splitting tensile tests according to EN 12390 were carried out, yielding  $f_{cm,cyl} = 9.76$  MPa and  $f_{ctm,sp,cyl} = 1.23$  MPa (with standard deviations of 5.59 and 0.55 MPa, respectively).

Direct shear tests were performed with a Wille Geotechnik test setup (see Figure 1) designed for rectangular specimens with maximum dimensions of  $(200 \times 205 \times 210)$  mm<sup>3</sup>. The test setup was chosen for two reasons: firstly, it replicates the in-situ shear stress in real hydraulic structures, and secondly, due to its adaptability for testing specimens with deviating geometries like the appropriated drill-cores: joints can be aligned with the horizontal shear force by placing arbitrarily shaped specimens in rectangular molds, which are subsequently filled with gypsum prior the direct shear testing. At the start of each test, the initial normal stress of  $\sigma_n = 0.5$  MPa, which was selected as representative for hydraulic structures, was applied. The normal force was kept constant during the experiment. Shear rate was  $\dot{v} = 0.1$  mm/min. Relative displacements and forces parallel and normal to the shear plane were recorded at 10 Hz.

## 3 | ANALYTICAL PROCEDURE AND RESULTS

The results of the shear tests were processed for obtaining shear ( $\sigma_v(v)$ ) and normal stresses ( $\sigma_n(v)$ ) as well as the dilation  $w(v)$ . Two distinctive types of result were found, depending on the shear bond state. Uncracked specimens with intact adhesion showed a peak shear stress before declining to a residual shear stress (Figure 3, left). Cracked specimens, where the adhesive bond had been

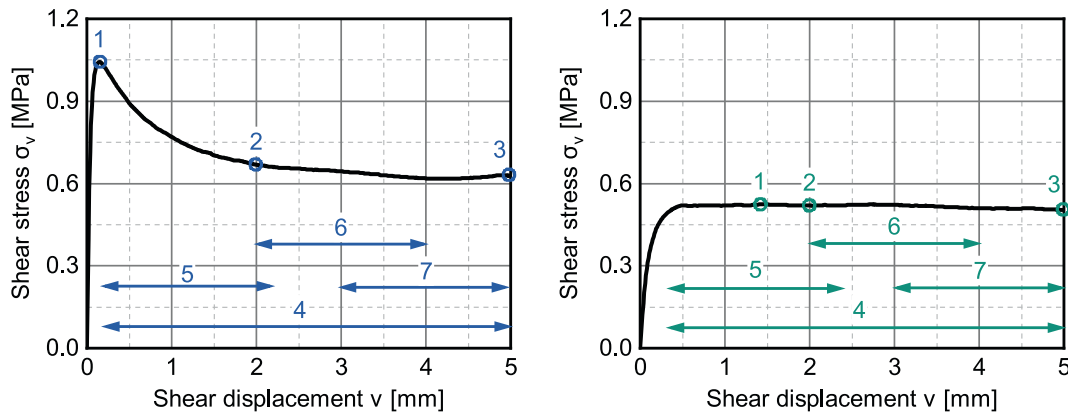


FIGURE 3 Shear stress curves of an uncracked specimen with intact adhesion (left) and of a cracked specimen without adhesion (right) including indication of modeling approaches 1–7.

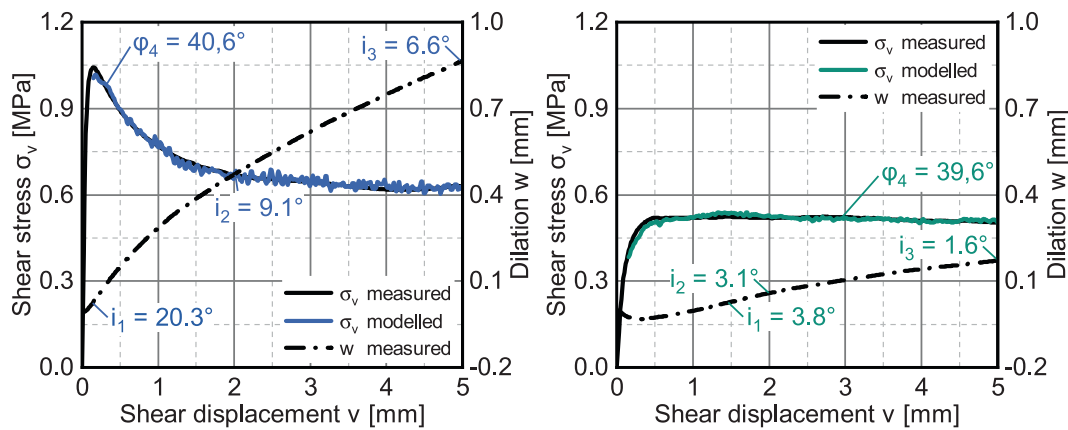


FIGURE 4 Dilation curves of an uncracked specimen with intact adhesion (left) and of a cracked specimen without adhesion (right) with subsequently modeled shear stress curves obtained from evaluation method 4. Shear tests corresponding to Figure 3.

destroyed before the sampling, exhibited a fast rise to a near constant shear stress or, in case of aggregate interlock, a comparatively small peak (Figure 3, right). Dilation curves were in general independent on shear bond state. After a small initial compression, monotonous dilation could be observed for most specimens (see Figure 4). Only the slope varied between tests, with cracked joints generally exhibiting smaller dilations, which even declined for high shear deformations in a few tests.

The applicability of Equation (3) for assessing the shear transfer behavior of joints in hydraulic structures was investigated by evaluating several singular values and sections of the shear stress curves (Figure 3). Singular values were the maximum shear stress,  $\sigma_{v,max}$  (1), an intermediate value at a shear deformation of  $v = 2$  mm (2) and at a shear deformation of  $v = 5$  mm (3). Sections were defined as the total shear stress curve (4),  $\Delta v = 2$  mm following peak shear stress (5) and the penultimate (6) and ultimate  $\Delta v = 2$  mm (7) of the shear test.

Figure 4 shows dilation curves  $w(v)$  corresponding to the shear stress curves in Figure 3. In the first evaluation

step, dilation angles  $i(v)$  were calculated through Equation (3). For the evaluation of singular values (1–3), friction angles  $\varphi$  were subsequently obtained from Equation (6).

$$\varphi = \arctan \frac{\sigma_v(v)}{\sigma_n(v)} - \arctan \frac{dw(v)}{dv} \quad (6)$$

Sectoral values of  $\varphi$  (4–7) were determined iteratively using the least-squares method (Equation (7)), with  $v_1$  and  $v_2$  varying depending on the evaluation method.

$$\min_{\varphi} \left( \int_{v_1}^{v_2} (\sigma_v(v) - \sigma_{v,mod}(v))^2 dv \right) \quad \text{with} \quad (7)$$

$$\sigma_{v,mod}(v) = \sigma_n(v) \times \tan \left( \varphi + \arctan \frac{dw(v)}{dv} \right)$$

Friction and dilation angles obtained from the shear tests are presented in Figure 5. The left diagram depicts

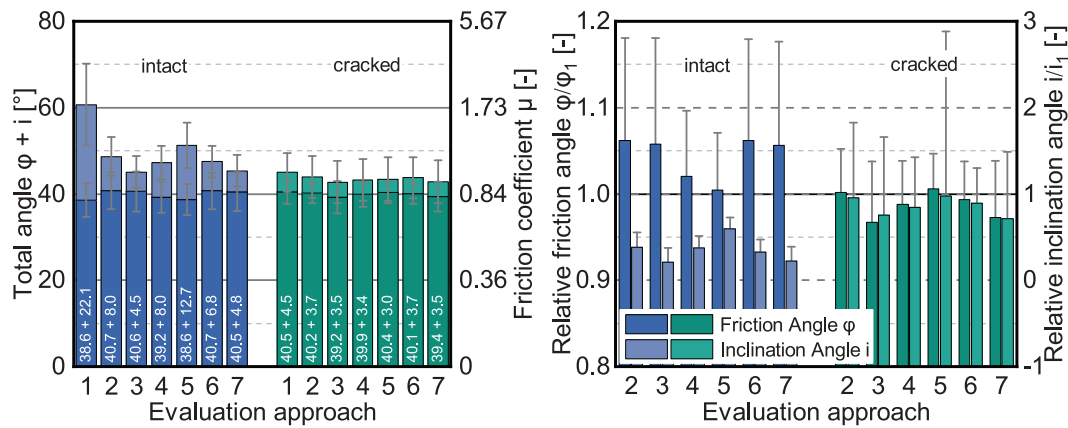


**FIGURE 5** Left: Average inclination angles  $i$  and friction angles  $\varphi$  with respective standard deviations of intact and cracked specimens for each evaluation method (definitions in Figure 3).

the absolute averages and respective standard deviations, distinguishing evaluation approaches as well as intact and cracked specimens. The diagram on the right shows relative angles, where the values for friction and inclination were compared to the respective angles at peak shear stress ( $\varphi_1, i_1$ ) before calculating averages of all tests for the remaining evaluation methods.

Average dilation angles of cracked concrete do not differ substantially between evaluation approaches. However, when evaluating individual shear tests, relative inclination can vary greatly, becoming even negative for some instances. For joints with intact bond, dilation angles are highest at peak shear stress and gradually decline with higher shear deformation  $v$ . In general, intact specimens show higher inclination angles through all evaluation methods.

The friction angles obtained from all evaluation approaches show rather uniform results for both intact and cracked specimens. However, when regarding relative friction angles,  $\varphi$  of intact specimens generally increases with rising shear deformation, while  $\varphi$  of cracked specimens declines—always considering the high standard deviations that complicate the comparison. Average friction angles of  $\varphi \approx 40^\circ$  disagree with results found in literature, where  $\phi$  lies in the range of  $22^\circ$  to  $27^\circ$ .<sup>13,23,24</sup> Friction angles of limestone, which were obtained by similar tests at similar normal stresses lie between  $33^\circ$  and  $40^\circ$ ,<sup>25</sup> while friction angles of rock-concrete joints are marginally higher with  $35^\circ$ ,  $39^\circ$ , and  $45^\circ$ .<sup>4,6</sup>

Figure 6 allows for a more in-depth analysis of the measured angles at peak shear stress. For the shear behavior of rock, a linear dependency of the total angle  $\varphi + i = \arctan \frac{\sigma_v}{\sigma_n}$  on the inclination angle,  $i$ , was found, thus confirming theory. Present results show this linearity to only be valid for inclination angles  $i < 30^\circ$ . For

higher inclination angles, caused by rougher surface topology, peak shear stress is overestimated and aggregate interlock has to be considered. The parameters influencing this breaking point require further research.

In addition to being influenced by inclination,  $\varphi$  also shows a dependency on stress level<sup>7;3</sup>. Figure 7 depicts the ratio of the friction angles following peak shear stress,  $\varphi_5$ , and at the end of the shear test,  $\varphi_7$  over peak shear stress,  $\sigma_{v,1}$  (for definitions see Figure 3). In general, it should be expected that by shearing-off of surface asperities, accumulating particles lead to a ball-bearing effect, thus continuously reducing friction and resulting in a friction angle ratio of  $\frac{\varphi_5}{\varphi_7} > 1$ . This could only be confirmed for low peak shear stresses. At high shear stresses, the stress dependency of the friction angle prevails, thus emphasizing the issue of friction mobilization at high shear stresses.

When comparing singular values in Figure 5 to their sectoral counterparts, they show a good equivalency, despite singular values are generally expected to be more prone to scattering. For being easier to obtain, singular values provide a sufficient quality of analysis. Sectoral evaluation methods, however, allow for an assessment of the quality of computed values.

Since sectoral friction angles are obtained by using the least-squares method on certain sections of the stress-deformation curve, they cannot be expected to fit the entire curve, especially when considering the aforementioned observations. For the evaluation of a hydraulic structure, the assumption of a constant average friction angle is beneficial, but requires an assessment method. Equations (8) and (9) propose an energy-based concept. As a first step the difference of the measured and the modeled shear stress curves is calculated and subsequently integrated over the shear deformation. The integrated difference is then normalized on the area under

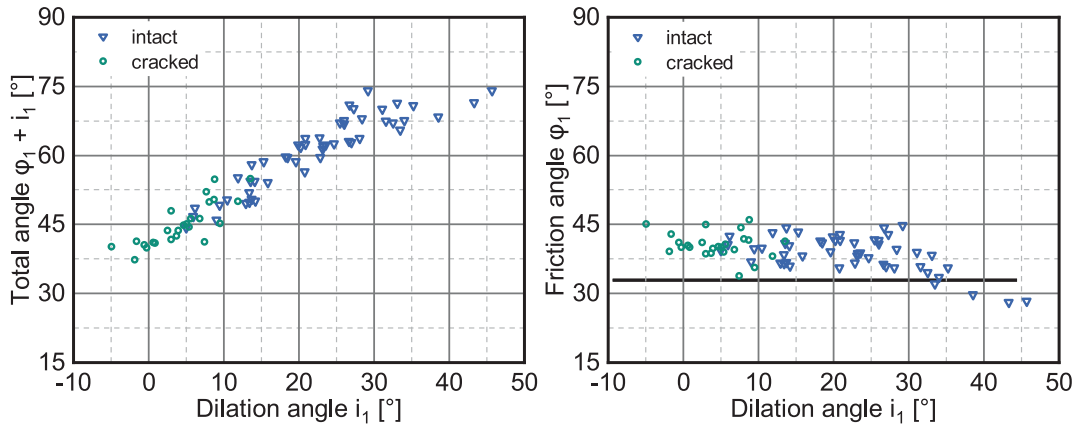


**FIGURE 6** Total angles  $\varphi + i = \arctan \frac{\sigma_v}{\sigma_n}$  (left) and friction angles  $\varphi_1$  (right) over dilation angles  $i_1$  measured at peak shear stress (evaluation method 1).

the shear stress-deformation curve, thereby accounting for different stress levels and maximum deformations, which allows a comparison of different shear tests. In Equation (8) the stress difference is entered as absolute values, thereby assessing the general fit and suitability of the model through the absolute deviation  $\delta_a$ . Equation (9) uses the real difference for calculating the total deviation  $\delta$ , which permits the subsequent assessment of whether the model over- or underestimates the measured stresses, as is relevant for structural integrity assessments.

$$\delta_a = \frac{\int_v |\sigma_v(v) - \sigma_{v,mod}(v)| dv}{\int_v \sigma_v(v) dv} \quad (8)$$

$$\delta = \frac{\int_v (\sigma_v(v) - \sigma_{v,mod}(v)) dv}{\int_v \sigma_v(v) dv} \quad (9)$$

Figure 8 shows the evaluation of Equations (8) and (9) for the sectoral approaches. Most shear tests performed well with only a few modeled stress curves absolutely deviating more than 10% from measurements. Evaluation approaches 4 and 6 (compare Figure 3) provide lower deviations than approaches 5 and 7, where changes of the friction angles effect the results. On the other hand, evaluation approach 6 and 7 tend to overestimate shear stress ( $\delta < 0$ ), while approaches 5 and—to a smaller degree—4 are more conservative. Generally, all tendencies are more pronounced for previously intact specimens. By setting limits for  $\delta_a$  and  $\delta$ , Equations (8)

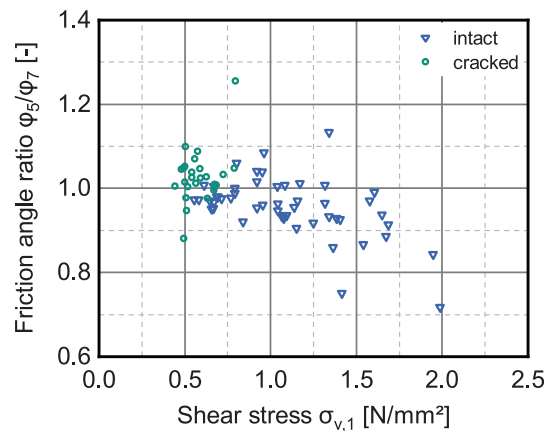


**FIGURE 7** Ratio of calculated friction angles following peak shear stress,  $\varphi_5$ , and at the end of the shear test,  $\varphi_7$  over peak shear stress,  $\sigma_{v,1}$  (definitions in Figure 3).

and (9) can be used for objectively identifying outliers or deciding whether a shear test result can be used for the structural assessment.

## 4 | SUMMARY AND OUTLOOK

The general evaluation method of concrete shear tests by separating the shear transfer behavior into friction and inclination was shown to be a useful tool for assessing joints in unreinforced concrete hydraulic structures for the experiments performed.

Using singular values of shear transfer parameters was shown to provide satisfactory results for analysis. Sectoral values—especially taking the entire stress-deformation-curve into consideration—provide more reliable results and permit an objective assessment of the quality

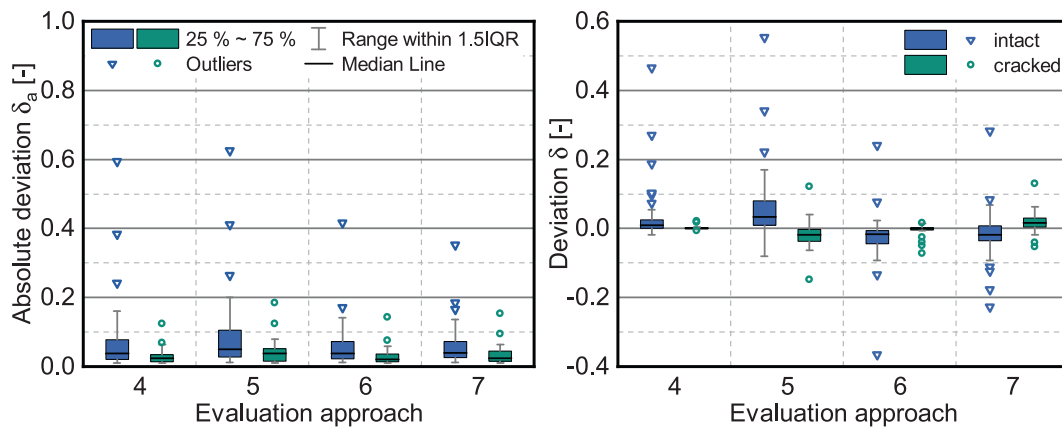


**FIGURE 8** Standardized deviations between modeled and measured shear stresses. Left: Absolute deviations according to Equation (8), right: deviations according to Equation (9).

of individual test results for statistically sound structural evaluations. The separation also allows for the determination of design values for distinct shear transfer parameters in future applications.

Subsequent research may focus on influencing parameters on either mechanism—friction and inclination—separately, for example, concrete composition or interface condition, especially since the presented research does not allow for establishing a connection between the shear transfer behavior and the individual surface topology (compare Equations (4) and (5)), due to the high scatter of the compressive strength. For hydraulic structures, the degradation of shear resistance over time following corrosion requires special focus.

Moreover, as hydraulic structures were the focus of the presented research, the advancement of the developed evaluation method, for example, based on a modified Mohr-Coulomb criterion,<sup>26</sup> for analyzing the shear transfer behavior of concrete joints with different properties is expedient. This requires the variation of concrete strength, interface roughness or normal stress, which was forgone in the presented investigation due to the specific goal of developing an evaluation method.

### FUNDING INFORMATION

Federal Ministry for Digital and Transport: BMVI-Expertennetzwerk Wissen—Können—Handeln, Grant Number: B3951.03.04.70014.

### DATA AVAILABILITY STATEMENT

The data that support the findings of this study are available from the corresponding author upon reasonable request.

### ORCID

Jan P. Höffgen  <https://orcid.org/0000-0003-1115-282X>

### REFERENCES

- DIN EN 1992-1-1:2011-01. Eurocode 2: design of concrete structures—Part 1-1: general rules and rules for buildings. German Version EN 1992-1-1:2004 + AC:2010, 2011. <https://doi.org/10.31030/1723945>
- fib 2013, *fib model code for concrete structures 2010*, Ernst & Sohn. <https://doi.org/10.1002/9783433604090>
- Schneider HJ. The laboratory direct shear test—an analysis and geotechnical evaluation. *Bull. Eng. Geol. Environ.* 1978; 18(1):121–6. <https://doi.org/10.1007/BF02635357>
- Saiang D, Malmgren L, Nordlund E. Laboratory tests on shotcrete-rock joints in direct shear, tension and compression. *Rock Mech Rock Eng.* 2005;38(4):275–97. <https://doi.org/10.1007/s00603-005-0055-6>
- Barton N. Shear strength criteria for rock, rock joints, rockfill and rock masses: problems and some solutions. *J Rock Mech Geotech Eng.* 2013, ISSN 16747755;5(4):249–61. <https://doi.org/10.1016/j.jrmge.2013.05.008>
- Tian HM, Chen WZ, Yang DS, Yang JP. Experimental and numerical analysis of the shear behaviour of cemented concrete-rock joints. *Rock Mech Rock Eng.* 2014;48(1):213–22. <https://doi.org/10.1007/s00603-014-0560-6>
- Höffgen JP, Haist M, Malárics-Pfaff V, Reschke T, Fleischer H, Müller HS, et al. Shear-friction behavior of non-reinforced concrete joints at low normal stresses. In: Ludwig H-M, Fischer H-B, Tagungsbericht I, editors. 20. Internationale Baustofftagung. Weimar; 2018. p. 1064–71, Weimar, Bundesrepublik Deutschland, F. A. Finger-Institut für Baustoffkunde, Bauhaus-Universität Weimar ISBN 3000599509.
- EN ISO 17892-10:2019-04. Geotechnical investigation and testing—laboratory testing of soil—Part 10: direct shear tests (ISO 17892-10:2018). German Version EN ISO 17892-10:2018, 2019. <https://doi.org/10.31030/2886159>
- Kelen N. Versuche zur Bestimmung des tangentialen Sohlwiderstandes von Gewichtsstaumauern. Berlin; 1933 (in German).
- Nissen I. Rißverzahnung des Betons: Gegenseitige Rißuferverschiebungen und übertragene Kräfte. Dissertation: Technische Universität München, München; 1987 (in German).

11. Saucier F, Bastien J, Pigeon M, Fafard M. A combined shear-compression device to measure concrete-to-concrete bonding. *Exp Tech*, vol. September/October. 1991;50–5.
12. Reinecke R. Haftverbund und Rissverzahnung in unbewehrten Betonschubfugen. Dissertation: Technische Universität München, München; 2004 (in German).
13. Wong RCK, Ma SKY, Wong RHC, Chau KT. Shear strength components of concrete under direct shearing. *Cem Concr Res*. 2007, ISSN 00088846;37(8):1248–56. <https://doi.org/10.1016/j.cemconres.2007.02.021>
14. Martin F-A, Rivard P. Effects of freezing and thawing cycles on the shear resistance of concrete lift joints. *Can J Civil Eng*. 2012, ISSN 0315-1468;39(10):1089–99. <https://doi.org/10.1139/l2012-090>
15. Mohamad ME, Ibrahim IS, Abdullah R, Abd Rahman AB, Kueh ABH, Usman J. Friction and cohesion coefficients of composite concrete-to-concrete bond. *Cem Concr Compos*. 2015, ISSN 09589465;56:1–14. <https://doi.org/10.1016/j.cemconcomp.2014.10.003>
16. Mattock AH, Hawkins NM. Shear transfer in reinforced concrete—recent research. *PCI J*. 1972;17(2):55–75. <https://doi.org/10.15554/pci.03011972.55.75>
17. Walraven JC. Aggregate interlock: a theoretical and experimental analysis. Dissertation. Delft: Delft University of Technology; 1980 <http://resolver.tudelft.nl/uuid:c33a2890-f9c1-4176-929e-6988f0f23640>
18. Randl N. Untersuchungen zur Kraftübertragung zwischen Alt- und Neubeton bei unterschiedlichen Fugenrauigkeiten. Dissertation: Technische Universität Innsbruck, Innsbruck; 1997 (in German).
19. Xia J, Shan K-Y, Wu X-H, Gan R-L, Jin W-L. Shear-friction behavior of concrete-to-concrete interface under direct shear load. *Eng Struct*. 2021, ISSN 01410296;238:112211. <https://doi.org/10.1016/j.engstruct.2021.112211>
20. Tse R, Cruden DM. Estimating joint roughness coefficients. *Int. J. Rock Mech. Min*. 1979, ISSN 01489062;16(5):303–7. [https://doi.org/10.1016/0148-9062\(79\)90241-9](https://doi.org/10.1016/0148-9062(79)90241-9)
21. Zhang X, Jiang Q, Chen N, Wei W, Feng X. Laboratory investigation on shear behavior of rock joints and a new peak shear strength criterion. *Rock Mech Rock Eng*. 2016, ISSN 0723-2632;49(9):3495–512. <https://doi.org/10.1007/s00603-016-1012-2>
22. Reschke T, Malárics-Pfaff V, Fleischer H, Höffgen JP. Scherfestigkeit von Beton und Mauerwerk an bestehenden Wasserbauwerken. FuE-Abschlussbericht, Bundesanstalt für Wasserbau. 2019; Karlsruhe, BAW-Nr. 3951.03.04.70014. (in German).
23. Waubke NV, Weiß R. Versuch zur Ermittlung der Haftreibung zwischen Betonoberflächen. *Cem Concr Res*. 1979;9(5):553–62. [https://doi.org/10.1016/0008-8846\(79\)90139-X](https://doi.org/10.1016/0008-8846(79)90139-X) ISSN 00088846. (in German).
24. Walraven JC, Reinhardt H-W. Theory and experiments on the mechanical behaviour of cracks in plain and reinforced concrete subjected to shear loading. *Heron*. 1981;26(1A): 1–68.
25. Barton N. The shear strength of rock and rock joints. *Int J Rock Mech*. 1976, ISSN 01489062;13(9):255–79. [https://doi.org/10.1016/0148-9062\(76\)90003-6](https://doi.org/10.1016/0148-9062(76)90003-6)
26. Randl N, Zilch K, Müller A. Bemessung nachträglich ergänzter Betonbauteile mit längsschubbeanspruchter Fuge. Vergleichende Beurteilung aktueller Konzepte für die Baupraxis. *Beton Stahlbetonbau*. 2008;103(7):482–97. <https://doi.org/10.1002/best.200800627> ISSN 00059900. (in German).

## AUTHOR BIOGRAPHIES



**Jan P. Höffgen:** Karlsruhe Institute of Technology, Institute of Concrete Structures and Building Materials, Karlsruhe, 76131, Germany. [jan.hoeffgen@kit.edu](mailto:jan.hoeffgen@kit.edu).



**Viktória Malárics-Pfaff:** Federal Waterways Engineering and Research Facility, Structural Engineering, Karlsruhe, 76187, Germany.



**Doris B. Wengrzik:** Karlsruhe Institute of Technology, Institute of Concrete Structures and Building Materials, Karlsruhe, 76131, Germany.



**Frank Dehn:** Karlsruhe Institute of Technology, Institute of Concrete Structures and Building Materials, Karlsruhe, 76131, Germany.

**How to cite this article:** Höffgen JP, Malárics-Pfaff V, Wengrzik DB, Dehn F. Analysis and evaluation of direct shear tests on concrete joints in hydraulic structures. *Structural Concrete*. 2023. <https://doi.org/10.1002/suco.202200797>